Electronic Structure of Ruthenium(II) Polyynyl Complexes

Olivia F. Koentjoro,[†,‡] Roger Rousseau,*[,†] and Paul J. Low*[,‡]

Steacie Institute for Molecular Sciences, 100 Sussex Drive, Ottawa, Ontario, K1A 0R6, Canada, and Department of Chemistry, University of Durham, South Road, Durham, DH1 3LE, U.K.

Received April 11, 2001

The electronic structure of the polyynyl complexes $[Ru\{(C{\equiv}C)_nR\}(PH_3)_2Cp]$ ($n = 1-6$; R = H, CH_3, C_6H_5, $C_6H_4NH_2$-*p*, $C_6H_4NO_2$-*p*, CN), the diynyl compounds $[Ru\{(C{\equiv}C)_2R\}(CO)_2Cp]$, and the oxidized species $[Ru\{(C{\equiv}C)_nC_6H_5\}(PH_3)_2Cp]^+$ have been studied using DFT methods. The optimized geometries are in good agreement with the few experimental structures available. The electronic structures are best described in terms of a strong σ-bonding component and a weaker interaction between the filled metal d orbitals and filled polyyne π orbitals. The charge distribution in the molecules and the energies and localization of the frontier orbitals have been examined to help rationalize the reactivity patterns emerging for this important class of compounds.

Introduction

Organometallic complexes of polyynyl $[(C{\equiv}C)_nR]$, polyyndiyl $[(C{\equiv}C)_n]$, polyenylidene $[(=C)_nR_2]$, and polyendiylidene $[(=C)_n=]$ ligands, which are highly unsaturated analogues of the well-known acetylide and carbene ligands, have been extensively investigated in recent times. The electronic properties of metal complexes bearing cumulated carbon ligands of various lengths (i.e., $\{C{=}C\}_n$) have been summarized in several recent reviews[1] and a notable piece of theoretical work,[2] and the electronic structures of several diyndiyl complexes have also been thoroughly studied.[3] Furthermore, the bonding of a monoynyl (or acetylide) ligand to a transition metal fragment is well established and best described in terms of overlap of the sp-hybridized σ orbital of the $[C{\equiv}CR]^-$ fragment with a metal fragment orbital of similar symmetry, usually composed of a large metal d-orbital component.[4] While a small metal-to-ligand back-bonding contribution may be identified, the most significant π-orbital mixings in this class of compounds arise from filled−filled interactions between the metal dπ orbitals and the occupied ligand π orbitals.

Several studies have employed vibrational spectroscopy to probe the electronic effects of σ-bonded polyynyl ligands on metal centers,[5,6] although these data reflect the *net* electronic effect of the polyynyl ligand and cannot distinguish a progressive increase in metal → π-ligand back-bonding interactions, arising from lower ligand π^* levels, from a progressively weaker σ-donating effect, which is in keeping with acidity measurements of the free polyynes.[7] Similarly, attempts to derive electronic information from structural data have not been conclusive, since the length of a C≡C bond is an unreliable measure of bond order and the available X-ray data are often of poor quality.[5a,c,8−10]

Lichtenberger and his colleagues have established the electronic structure of $Fe(C{\equiv}CC{\equiv}CH)(CO)_2Cp$ using He(I) and He(II) photoelectron spectroscopy (PES) together with Fenske−Hall and EHMO calculations.[11] The Fe−C σ bond was found to be formed by donation from the diynyl σ_{sp} orbital into an empty metal d_{z^2} orbital, while the most significant π-type interactions occur between the set of occupied diynyl π e levels and occupied metal dπ orbitals. As a result of this filled−filled (or four-electron, two-orbital) π interaction between the ligand and the metal, the HOMO contained considerable diynyl π character. The empty π^* orbitals

* Corresponding authors. (R.R.) E-mail: roger@ned1.sims.nrc.ca. Fax: +(1) 613 947 2838. (P.J.L.) E-mail p.j.low@durham.ac.uk. Fax: +(44) (0)191 384 4737.
† Steacie Institute.
‡ University of Durham.

(1) Bruce, M. I.; Swincer, A. G. *Adv. Organomet. Chem.* **1983**, *22*, 59. (b) Bruce, M. I. *Chem. Rev.* **1991**, *91*, 197. (c) Bruce, M. I. *Chem. Rev.* **1998**, *98*, 2797.

(2) Re, N.; Sgamellotti, A.; Floriani, C. *Organometallics* **2000**, *19*, 1115.

(3) (a) Bruce, M. I.; Low, P. J.; Costuas, K.; Halet, J.-F.; Best, S. P.; Heath, G. A. *J. Am. Chem. Soc.* **2000**, *122*, 1949. (b) Brady, M.; Weng, W.; Zhou, Y.; Seyler, J. W.; Amoroso, A. J.; Arif, A. M.; Boehme, M.; Frenkling, G.; Gladysz, J. A. *J. Am. Chem. Soc.* **1997**, *119*, 775. (c) Le Narvor, N.; Toupet, L.; Lapinte, C. *J. Am. Chem. Soc.* **1995**, *117*, 1825. (d) Kheradmandan, S.; Heinze, K.; Schmalle, H. W.; Berke, H. *Angew. Chem., Int. Ed.* **1999**, *38*, 2270.

(4) (a) McGrady, J. E.; Lovell, T.; Stranger, R.; Humphrey, M. G. *Organometallics* **1997**, *16*, 4004. (b) John, K. D.; Stoner, T. C.; Hopkins, M. D. *Organometallics* **1997**, *16*, 4948. (c) Kostic, N. M.; Fenske, R. F. *Organometallics* **1982**, *1*, 974. (d) Beddoes, R. L.; Bitcon, C.; Whiteley, M. W. *J. Organomet. Chem.* **1991**, *402*, 85. (e) Bruce, M. I.; Humphrey, M. G.; Snow, M. R.; Tiekink, E. R. T. *J. Organomet. Chem.* **1986**, *314*, 213. (f) Lichtenberger, D. L.; Gruhn, N. E.; Renshaw, S. K. *J. Mol. Struct.* **1997**, *405*, 79.

(5) ν(CO): (a) Akita, M.; Chung, M.-C.; Sakurai, A.; Sugimoto, S.; Terada, M.; Tanaka, M.; Moro-oka, Y. *Organometallics* **1997**, *16*, 4882. (b) Coat, F.; Guillevic, M.-A.; Toupet, L.; Paul, F.; Lapinte, C. *Organometallics* **1997**, *16*, 5988. (c) Sun, Y.; Taylor, N. J.; Carty, A. J. *Organometallics* **1992**, *11*, 4293. (d) Wong, A.; Kang, P. C. W.; Tagge, C. D.; Leon, D. R. *Organometallics* **1990**, *9*, 1992. ν(NO): (e) Dembinski, R.; Bartik, T.; Bartik, B.; Jaeger, M.; Gladysz, J. A. *J. Am. Chem. Soc.* **2000**, *122*, 810.

(6) Markwell, R. D.; Butler, I. S.; Kakkar, A. K.; Khan, M. S.; Al-Zakwani, Z. H.; Lewis, J. *Organometallics* **1996**, *15*, 2331.

(7) Eastmond, R.; Johnson, T. R.; Walton, D. R. M. *J. Organomet. Chem.* **1973**, *50*, 87.

(8) (a) Manna, J.; John, K. D.; Hopkins, M. D. *Adv. Organomet. Chem.* **1995**, *38*, 79. (b) Low, P. J.; Bruce, M. I. *Adv. Organomet. Chem.* **2001**, *48*, 71.

10.1021/om010304+ CCC: $20.00
Publication on Web 09/25/2001

Chart 1. Compounds and Atom Labeling Scheme Associated with the Polyynyl Ligand Used in This Work

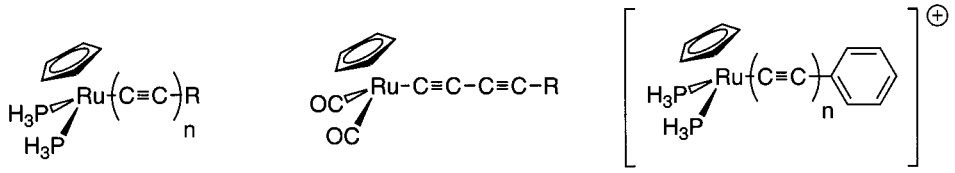

(**1**) (**2**) (**3**)

n =1-6

R = H, CH_3, C_6H_5, $C_6H_4NH_2$-*p*, $C_6H_4NO_2$-*p*, CN

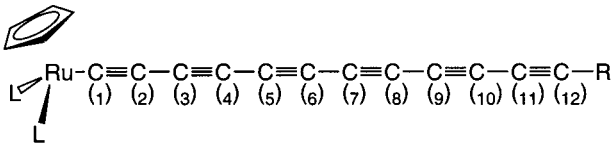

of the $[C{\equiv}CC{\equiv}CH]^-$ fragment were found some 13.9 eV above the occupied orbitals of similar symmetry, and consequently the π-acceptor character of the [C≡CC≡CH] ligand is negligible.[11]

Prompted by recent synthetic work[10] and given the interest in polyynyl complexes as potential components for molecular scale wires[12] and NLO active materials,[13] we have examined the electronic structure of a series of complexes $[Ru\{(C{\equiv}C)_nR\}(PH_3)_2Cp]$ ($n = 1-6$) (**1**) and $[Ru\{(C{\equiv}C)_2R\}(CO)_2Cp]$ (**2**), which feature end-capping groups R with a range of electronic properties (R = H, CH_3, C_6H_5, $C_6H_4NH_2$-*p*, $C_6H_4NO_2$-*p*, CN) and also the oxidized compounds $[Ru\{(C{\equiv}C)_nPh\}(PH_3)_2Cp]^+$ ($n = 1-6$) (**3**) (Chart 1).

Computational Methods

Geometry optimization and orbital calculations were performed using the B3LYP functional[14] as implemented within the Gaussian 98 software package,[15] with a 3-21G* basis set for ruthenium and a 6-31G** basis set for all other atoms. We tested these conclusions against the LanL2DZ basis set used in our previous work and found consistent trends in bond distances and charge distributions with only small variations in the absolute values of these parameters (0.03 Å in bond length and 0.05 e in charge).[16] Default criteria within the software were employed for geometry optimization, which places an uncertainty of less than ±0.005 Å on bond lengths. C_s symmetry is imposed on both electronic and nuclear degrees of freedom during optimization, and no stationary point analysis was performed. Population analysis was performed within the formalization of natural orbitals.[17] Although this charge analysis is not in any way unique, it does allow us to report relative charges that are not sensitive to basis set, as is the case for Muliken population, and thus the results are consistent whether a minimal or extended basis set is used. For the case of oxidized species the structures were fully optimized using the unrestricted open shell formalism. The deviation of the electronic state from a pure doublet was minimal, as measured by values of the spin operator S where the maximum deviation from $S^2 = 0.75$ (pure doublet) was found to be at most 0.01, indicating negligible spin contamination. As a complementary approach, we have also performed a fragment orbital analysis with the Amsterdam Density Functional Program (ADF), and the double-ζ basis set included with the package was employed for all atoms.[18] Here we employ the Becke Perdew-86 functional combination, which provides Kohn−Sham orbitals in excellent agreement with the B3LYP orbitals obtained from Gaussian 98.[19] Finally, the results of the orbital calculations were displayed graphically using Molekel.[20]

Results and Discussion

Structure and Bonding. The geometries calculated for $[Ru\{(C{\equiv}C)_nC_6H_5\}(PH_3)_2Cp]$ ($n = 1, 2$) are in good agreement with the experimental structures of the PPh_3 analogues (Table 1).[10,21] Complete agreement between

(9) For examples see Ti: (a) Hayashi, Y.; Osawa, M.; Kobayashi, K.; Wakatsuki, Y. *Chem. Commun.* **1996**, 1617. (b) Hayashi, Y.; Osawa, M.; Wakatsuki, Y. *J. Organomet. Chem.* **1997**, *542*, 241. Zr: (c) Oberthur, M.; Hillebrand, G.; Arndt, P.; Kempe, R. *Chem. Ber./Recl.* **1997**, *130*, 789. W: (d) Bruce, M. I.; Ke, M.; Low, P. J.; Skelton, B. W.; White, A. H. *Organometallics* **1998**, *17*, 3539. Re: (e) Dembinski, R.; Lis, T.; Szafert, S.; Mayne, C. L.; Bartik, T.; Gladysz, J. A. *J. Organomet. Chem.* **1999**, *578*, 229. (f) Bartik, B.; Dembinski, R.; Bartik, T.; Arif, A. M.; Gladysz, J. A. *New J. Chem.* **1997**, *21*, 739. (g) Yam, V. W.-W.; Chong, S. H.-F.; Cheung, K.-K.; *Chem. Commun.* **1998**, 2121. (h) Yam, V. W.-W.; Chong, S. H. F.; Ko, C. C. *Organometallics* **2000**, *19*, 5092. Ru: (i) Romero, A.; Peron, D.; Dixneuf, P. H. *J. Chem. Soc., Chem. Commun.* **1990**, 1410. Os: (j) Werner, H.; Flugel, R.; Windmuller, B. *Chem. Ber./Recl.* **1997**, *130*, 493. Ni: (k) Gallagher, J. F.; Butler, P.; Manning, A. R. *Acta Crystallogr.* **1998**, *C54*, 342. Pt: (l) Marder, T. B.; Lesley, G.; Yaun, Z.; Fyfe, H. B.; Chow, P.; Stringer, G.; Jobe, I. R.; Taylor, N. J.; WIlliams, I. D.; Kurtz, S. K. *Materials for Nonlinear Optics. Chemical Perspectives*; ACS Symp. Ser. 455; 1991; Chapter 40. (m) AlQuaisi, S. M.; Galat, K. J.; Chai, M.; Ray, D. G., III; Rinaldi, P. L.; Tessier, C. A.; Youngs, W. J. *J. Am. Chem. Soc.* **1998**, *120*, 12149. Zn: (n) Krieger, M.; Gould, R. O.; Neumueller, B.; Harms, K.; Dehnicke, K. *Z. Anorg. Allg. Chem.* **1998**, *624*, 1434.

(10) Bruce, M. I.; Hall, B. C.; Kelly, B. D.; Low, P. J.; Skelton, B. W.; White, A. H. *J. Chem. Soc., Dalton Trans.* **1999**, 3719.

(11) Lichtenberger, D. L.; Renshaw, S. K.; Wong, A.; Tagge, C. D. *Organometallics* **1993**, *12*, 3522.

(12) Ward, M. D. *Chem. Ind.* **1996**, 568.

(13) Fyfe, H. B.; Klekuz, M.; Stringer, G.; Taylor, N. J.; Marder, T. B. NATO, ASI Series, Series E **1992**, *206*, 331.

(14) Becke, A. D. *J. Chem. Phys.* **1993**, *98*, 5648.

(15) Frisch, M. J.; Trucks, G. W.; Schlegel, H. B.; Scuseria, G. E.; Robb, M. A.; Cheeseman, J. R.; Zakrzewski, V. G.; Montgomery, J. A., Jr.; Stratmann, R. E.; Burant, J. C.; Dapprich, S.; Millam, J. M.; Daniels, A. D.; Kudin, K. N.; Strain, M. C.; Farkas, O.; Tomasi, J.; Barone, V.; Cossi, M.; Cammi, R.; Mennucci, B.; Pomelli, C.; Adamo, C.; Clifford, S.; Ochterski, J.; Petersson, G. A.; Ayala, P. Y.; Cui, Q.; Morokuma, K.; Malick, D. K.; Rabuck, A. D.; Raghavachari, K.; Foresman, J. B.; Cioslowski, J.; Ortiz, J. V.; Stefanov, B. B.; Liu, G.; Liashenko, A.; Piskorz, P.; Komaromi, I.; Gomperts, R.; Martin, R. L.; Fox, D. J.; Keith, T.; Al-Laham, M. A.; Peng, C. Y.; Nanayakkara, A.; Gonzalez, C.; Challacombe, M.; Gill, P. M. W.; Johnson, B. G.; Chen, W.; Wong, M. W.; Andres, J. L.; Head-Gordon, M.; Replogle, E. S.; Pople, J. A. *Gaussian 98*; Gaussian, Inc.: Pittsburgh, PA, 1998.

(16) Low, P. J.; Rousseau, R.; Lam, P.; Udachin, K. A.; Enright, G. D.; Tse, J. S.; Wayner, D. D. M.; Carty, A. J. *Organometallics* **1999**, *18*, 3885.

(17) Reed, A. E.; Curtiss, L. A.; Weinhold, F.; *Chem. Rev.* **1988**, *88*, 899.

Table 1. Bond Lengths Associated with the Metal−Polyynyl Portion of the Molecules [Ru{(C≡C)$_n$C$_6$H$_5$}(PH$_3$)$_2$Cp][a]

	n					
bond (Å)	1 (see ref 21)	2 (see ref 10)	3	4	5	6
Ru−C(1)	2.008 *2.016(3)*	1.988 *1.994(4)*	1.980	1.974	1.970	1.968
C(1)−C(2)	1.227 *1.215(4)*	1.233 *1.206(5)*	1.235	1.236	1.238	1.238
C(2)−C(3)		1.359 *1.389(6)*	1.350	1.347	1.344	1.342
C(3)−C(4)		1.223 *1.200(6)*	1.231	1.233	1.235	1.236
C(4)−C(5)			1.351	1.343	1.338	1.336
C(5)−C(6)			1.225	1.233	1.237	1.238
C(6)−C(7)				1.349	1.340	1.337
C(7)−C(8)				1.226	1.233	1.237
C(8)−C(9)					1.349	1.339
C(9)−C(10)					1.226	1.234
C(10)−C(11)						1.348
C(11)−C(12)						1.225
C(2*n*)−C$_6$H$_5$	1.427 *1.456(4)*	1.421 *1.416(6)*	1.420	1.419	1.419	1.420

[a] Experimental values are given in italics.

the metrical parameters of the optimized and experimental structures is not expected given the differences in supporting ligands (PH$_3$ vs PPh$_3$), the gas-phase nature of the computation, the relatively small basis set employed, and errors inherent within the functional. Nevertheless, the structural deviations, such as they are, fall well within 0.03 Å, giving confidence in the accuracy and relevance of the computed geometries described herein. For each of the complexes [Ru{(C≡C)$_n$C$_6$H$_5$}(PH$_3$)$_2$Cp] examined (n = 1−6), the C≡C bond length of the alkyne moiety directly attached to the phenyl group was remarkably invariant (1.22−1.23 Å), as were the C−C$_6$H$_5$ bond lengths (1.42−1.43 Å). As the polyynyl ligand is allowed to lengthen, a strict C≡C/C−C bond alternation pattern along the carbon chain emerges, with C≡C bond lengths falling in the range 1.22−1.24 Å, and C−C between 1.34 and 1.36 Å (Table 1). An examination of the parent polyynes [H(C≡C)$_n$H] showed similar trends in the C≡C and C−C bond lengths, with the parameters of the interior C≡C/C−C bonds approaching a limit of 1.23/1.34 Å with increasing n.[22] Thus the metal center plays little role in determining the bond lengths of the remote acetylenic moieties, and the small variations in structure are more an inherent property of the conjugated chain than a function of the metal center. Thus for the current purposes the most important feature of the computed structures of the [Ru{(C≡C)$_n$C$_6$H$_5$}(PH$_3$)$_2$Cp] series lies in the steady decrease in the Ru−C(1) bond length with increasing values of n (Table 1).

A simplified representation of the fragment orbital interaction diagram for [Ru(PH$_3$)$_2$Cp]$^+$ and [(C≡C)$_n$R]$^-$ (R = C$_6$H$_5$, n = 2 and 6) is presented in Figure 1. The lowest energy orbital of the [Ru(PH$_3$)$_2$Cp]$^+$ fragment is the $d_{x^2-y^2}$, which is the d orbital least destabilized by the interactions with the cyclopentadienyl and phosphine ligands. Locally, this orbital does not have the correct symmetry to interact with the polyyne chain orbitals and remains essentially nonbonding. The next highest metal fragment orbitals are the quasi-degenerate d_{xz} and d_{yz} pair, which are of correct symmetry to interact with a similar pair of quasi-degenerate orbitals on the [(C≡C)$_n$R]$^-$ fragment. For all [(C≡C)$_n$R]$^-$ species considered in this work these later orbitals invariably consist of $C_{p\pi}$ interactions which are bonding across bonds formally considered C≡C triple bonds and antibonding between those formally considered C−C single bonds. We denote this pair as π_x and π_y for brevity. These orbitals form a filled bonding and antibonding set with the d_{xz} and d_{yz} orbitals, the latter combination of which becomes the pair of quasi-degenerate HOMOs of the combined molecule. These HOMOs are only slightly stabilized by minor mixing (1−5%) with the next highest set of π orbitals (denoted π^*_x and π^*_y for simplicity) on the [(C≡C)$_n$R]$^-$ fragment. Thus to a first-order approximation, the $d_{xz}-\pi_x$ and $d_{yz}-\pi_y$ pairs may both be considered to be derived from four-electron two-orbital interactions. By far the strongest interaction occurs between the HOMO of the [(C≡C)$_n$R]$^-$ fragment, which is a σ-type lone pair (LP) orbital located on the terminal carbon, and the d_{z^2} orbital on Ru. This pair forms a strong bonding and antibonding pair, of which only the bonding combination is occupied. The highest metal d orbital is the d_{xy}, which, like the $d_{x^2-y^2}$, does not have the correct local symmetry to interact with the [(C≡C)$_n$R]$^-$ fragment orbitals and is thus nonbonding. Therefore, a simple description of the bonding between the [Ru(PH$_3$)$_2$Cp]$^+$ and [(C≡C)$_n$R]$^-$ fragments involves a Ru−C single bond and notes that the metal orbitals do not have a significant net interaction with the π orbitals of the polyynyl ligand. The presence of the metal fragment only introduces a weak perturbation effect on the polyyne fragment by inducing a minor mixing within the [(C≡C)$_n$R]$^-$ π orbitals. This scenario is in good qualitative agreement with previous studies of acetylide complexes,[4] the iron diynyl complex Fe(C≡CC≡CH)(CO)$_2$Cp,[11] and various diyndiyl complexes.[3]

The general features of the orbital interaction diagrams for both complexes are similar, save for a steady decrease in the energies of the frontier orbitals of the [(C≡C)$_n$R]$^-$ fragment, by about 2.5 eV between n = 2 and n = 6, due to the greater capacity of the longer polyynyl fragments to stabilize the negative charge. This steady decrease in isolobal frontier orbital energy occurs for both σ and π states and is largely attenuated beyond n = 4 for the C$_6$H$_5$ end cap: the n = 6 orbital energies are only 0.5 eV lower in energy then those for n = 4. This effect is strongly correlated with the nature of the end group where, in general, the more powerful electron-withdrawing groups stabilize the negative charge. For

(18) (a) ADF Program System Release 2000.02. Scientific computing and modelling NV; Vrije Universiteit; Theoretical Chemistry, De Boelelaan 1083, 1081 HV Amsterdam, The Netherlands. (b) Baerends, E. J.; Ellis, D. E.; Ros, P. *Chem. Phys.* **1973**, *2*, 41. (c) Versluis, L.; Zeigler, T. *J. Chem. Phys.* **1988**, *88*, 322. (d) te Velde, G.; Baerends, E. J. *J. Comput. Phys.* **1992**, *99*, 84. (e) Fonseca Guerra, C.; Snijders, J. G.; te Velde, G.; Caerends, E. J. *Theor. Chem. Acc.* **1998**, *99*, 391.

(19) (a) Becke, A. D. *Phys. Rev. A* **1988**, *38*, 2398. (b) Perdew, J. P. *Phys. Rev. B* **1986**, *33*, 8822. (c) Perdew, J. P. *Phys. Rev. B* **1986**, *B34*, 7046.

(20) Flükiger, P.; Lüthi, H. P.; Weber, J. *Molekel*, Revision 4.0; Swiss Center for Scientific Computing: Manno, Switzerland, 2000.

(21) Wisner, J. M.; Bartczak, T. J.; Ibers, J. A. *Inorg. Chim. Acta* **1985**, *100*, 115.

(22) Various computational studies have been performed on the R(C≡C)$_n$R series, and the data collected here are in good general agreement. See for example: (a) Hoffmann, R. *Tetrahedron* **1966**, *22*, 521. (b) Fan, Q.; Pfeiffer, G. V. *Chem. Phys. Lett.* **1989**, *162*, 472. (c) Schermann, G.; Grosser, T.; Hampel, F.; Hirsch, A. *Chem. Eur. J.* **1997**, *3*, 1105.

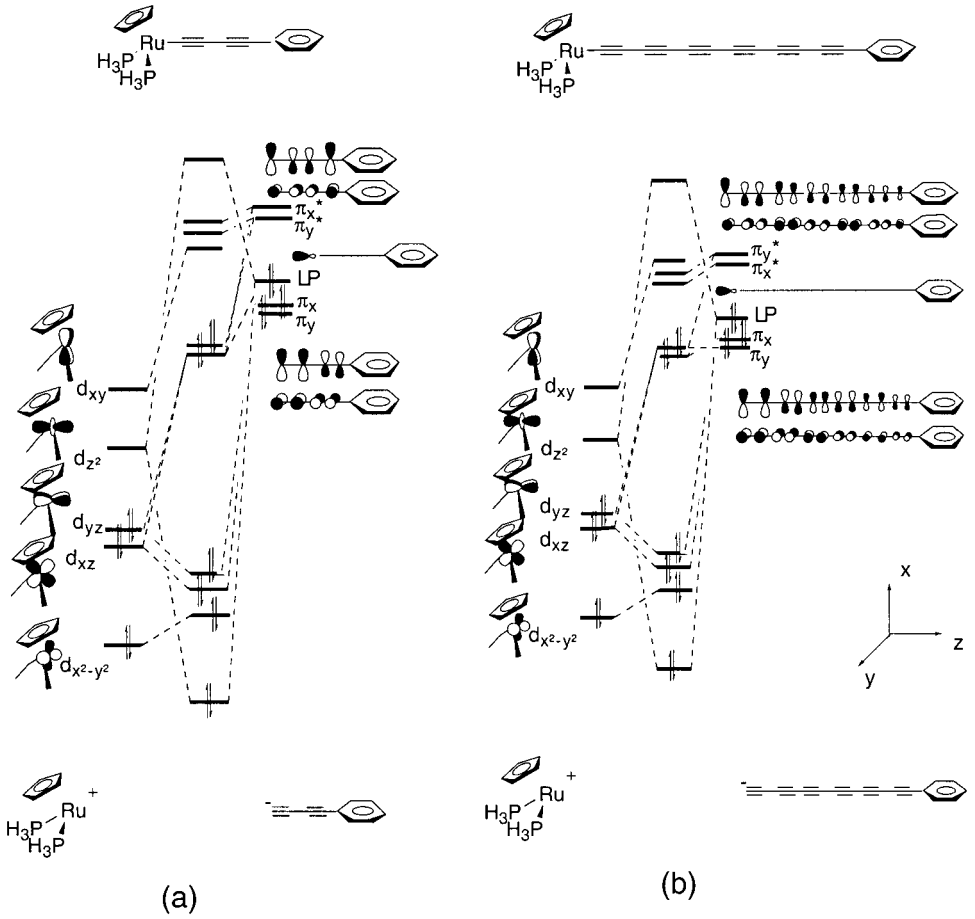

Figure 1. Schematic molecular orbital diagram for the complexes (a) [Ru{(C≡C)$_2$C$_6$H$_5$}(PH$_3$)$_2$Cp] and (b) [Ru{(C≡C)$_6$C$_6$H$_5$}-(PH$_3$)$_2$Cp] depicting the interactions between the frontier orbitals of [Ru(PH$_3$)$_2$Cp]$^+$ and [(C≡C)$_n$C$_6$H$_5$]$^-$.

example, the frontier orbitals of the [(C≡C)$_2$CN]$^-$ fragment are isolobal with those of the [(C≡C)$_n$C$_6$H$_5$]$^-$ series and roughly equivalent in energy to those of [(C≡C)$_6$-C$_6$H$_4$]$^-$. Likewise, there is a stabilization of about 1.5 eV for the orbitals of [(C≡C)$_6$CN]$^-$ relative to those of [(C≡C)$_2$CN]$^-$. Hence, the frontier orbitals of the polyynyl fragment can be stabilized by CN (or C$_6$H$_4$NO$_2$-*p*) groups to a greater extent then H or C$_6$H$_5$ end-caps, but the general trend of more stable fragment orbitals with increasing chain length is preserved. There is a substantial stabilization of the LUMO with increasing values of *n* due to the decreasing energy of the ligand π-type orbitals (Figure 1). The large energy gap that separates the occupied and unoccupied orbitals in the diynyl complex decreases with increasing chain length, and the composition of the LUMO shifts from being predominantly metal d$_{xy}$ in character to almost exclusively polyynyl (π^*_x and π^*_y) centered (Figure 2). Thus, increasing polynyl chain length has two major consequences upon the bonding to the [Ru(PH$_3$)$_2$Cp]$^+$ fragment. First, the σ donation of the LP orbital is less effective in transferring charge to the metal center. Second, the net contribution from the metal center to the HOMOs of the combined molecule is reduced for the longer polyynyl complexes (Figure 2).

In polyynyl complexes [Ru{(C≡C)$_n$R}(PH$_3$)$_2$Cp] containing the electron-donating end-caps (R = H, CH$_3$, and C$_6$H$_4$NH$_2$-*p*) the HOMO−LUMO gap decreases by approximately 1 eV as the chain is lengthened from one alkynyl moiety to six, while for the CN-capped series

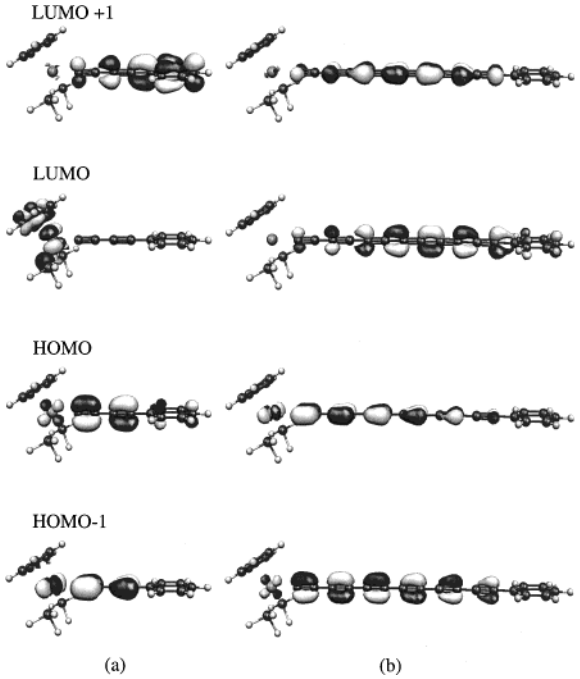

Figure 2. Iso-surface (0.005 au) plots of the frontier orbitals of (a) [Ru{(C≡C)$_2$C$_6$H$_5$}(PH$_3$)$_2$Cp] and (b) [Ru{(C≡C)$_6$C$_6$H$_5$}(PH$_3$)$_2$Cp].

the gap decreases by as much as 1.5 eV. A much smaller decrease in the HOMO−LUMO gap (0.5 eV) was found for the C$_6$H$_4$NO$_2$-*p* series, which is somewhat surprising given the similar electron-withdrawing power of the CN

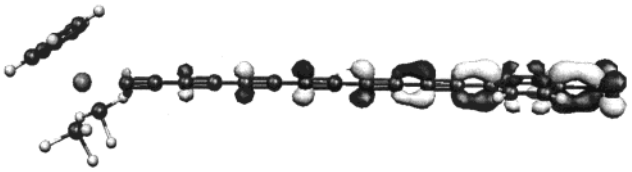

Figure 3. Iso-surface (0.005 au) plot of the LUMO of the nitrophenyl-substituted complex [Ru{(C≡C)$_2$C$_6$H$_4$NO$_2$-*p*}-(PH$_3$)$_2$Cp]; compare with Figure 2a.

Table 2. Computed Bond Order Associated with the Acetylide Ligand C≡C Triple Bond in the Substituted Complexes [Ru(C≡CR)(PH$_3$)$_2$Cp] (R = C$_6$H$_4$NH$_2$-*p*, CH$_3$, H, C$_6$H$_5$, C$_6$H$_4$NO$_2$-*p*, CN)

R	ρ bonding	ρ antibonding	BO
C$_6$H$_4$NH$_2$-*p*	5.86	0.22	2.82
H	5.97	0.14	2.91
CH$_3$	5.92	0.19	2.86
C$_6$H$_5$	5.85	0.22	2.82
C$_6$H$_4$NO$_2$-*p*	5.80	0.23	2.79
CN	5.78	0.27	2.75

and C$_6$H$_4$NO$_2$-*p* groups, but may be attributed to the significant contribution of the NO$_2$ group to the LUMO in this case (Figure 3). Therefore while the end-cap has a role in tuning the orbital energies, the electronic structure and orbital composition is grossly the same for all complexes examined in this study.

The possibility of cumulenic resonance contributors to the valence structure of di- and polyynyl complexes has been suggested to help explain some of the unusual spectroscopic and structural parameters observed for these complexes.[5a,c,23] To address this point, the computed bond orders, expressed as half the difference of the bonding and antibonding electron population as determined by natural bond order (NBO) analysis, for each of the C−C bonds for the alkynyl moiety in the series [Ru(C≡CR)(PH$_3$)$_2$Cp] (R = H, CH$_3$, C$_6$H$_5$, C$_6$H$_4$-NO$_2$-*p*, C$_6$H$_4$NH$_2$-*p*, CN) are given in Table 2. This parameter allows us to quantify the contribution of d−π interactions, which as indicated above *do* cause some remixing of the frontier orbitals of the polyynyl fragment, yet allows us to avoid unduly complicated descriptions that would undoubtedly arise from an analysis of mixing between many orbitals. The computed bond orders for the alkynyl moiety in the ynyl series [Ru(C≡CR)(PH$_3$)$_2$Cp] fall in the range 2.75 (R = CN) to 2.91 (R = H), with the general observation that electron-withdrawing end-caps induce the lowest C(1)≡C(2) bond orders. Almost all of the reduction in bond order comes from both a decrease in the population of carbon π-bonding orbitals and an *almost equivalent* increase in the population in the π*-antibonding orbitals. This polarization, or remixing, of the π electrons is the underlying reason for the increase of C≡C bond lengths observed in these molecules relative to acetylene. Thus, the observed trends in C(1)≡C(2) bond length may be rationalized in terms of a secondary remixing of the backbone π orbitals induced either by the metal fragment or by the nonmetal end group. As the polyynyl ligand chain length is increased from n = 1 to n = 6, there is a further decrease in the C(1)≡C(2) bond order [2.66 (R = CN) to 2.68 (R = C$_6$H$_5$)], which again arises from a combination of the decreased bonding density and a corresponding increase in the antibonding density. For the remaining C≡C bonds in the carbon backbone, the calculated bond orders fall within the range 2.56−2.78, similar to those within the parent molecule H(C≡C)$_6$H (2.61−2.65).

Table 3. Fragment Charges and Total Charge Distribution for [Ru{(C≡C)$_n$C$_6$H$_5$}(PH$_3$)$_2$Cp]

n	qRu(PH$_3$)$_2$-Cp (e$^-$)	q(C≡C)$_n$ (e$^-$)	qC$_6$H$_5$ (e$^-$)	qC$_{(1+2)}$ (e$^-$)	qC$_{(3-n)}$ (e$^-$)	% q C$_{(1+2)}$	% q C$_{(3-n)}$
1	0.50	−0.43	−0.07	−0.43		100	
2	0.54	−0.49	−0.05	−0.45	−0.05	91	9
3	0.56	−0.53	−0.03	−0.43	−0.10	81	19
4	0.57	−0.56	−0.01	−0.43	−0.14	76	24
5	0.59	−0.58	0.00	−0.42	−0.16	72	28
6	0.60	−0.60	0.00	−0.41	−0.19	68	32

Charge Distribution and Electrostatic Effects

To complement the orbital analysis outlined above, we examined the charge distribution within the [Ru{(C≡C)$_n$C$_6$H$_5$}(PH$_3$)$_2$Cp] series. Summation of the natural charge on each of the fragments [Ru(PH$_3$)$_2$Cp], [(C≡C)$_n$], and [C$_6$H$_5$] indicated a substantial amount of negative charge (−0.40 to −0.60 e) on the polyynyl chain, the majority of which resides on the alkyne moiety adjacent to the metal center due to the involvement of this moiety in the strong, polar covalent σ bond with the metal center (Table 3). The amount of charge distributed along the carbon chain is significantly larger than was found for the *p*-amino-*p*′-nitrodiphenyl alkyne systems (0.14 e), due to the presence of the metal center in the present work.[24] In agreement with our fragment orbital analysis, the larger n chains bear a greater negative charge, resulting in larger positive charge on both the [Ru(PH$_3$)$_2$Cp] and [C$_6$H$_5$] fragments (Table 3). The resulting increased Coulombic attraction between the metal and carbon fragments with increasing n is most likely responsible for the decreased Ru−C(1) bond length computed for the longer chain polyynyl complexes (Table 1).

Similarly, the total amount of charge deposited on the polyynyl chain is related not only to the length of the polyynyl ligand but also to the electronic nature of the nonmetal end-cap. As the nonmetal end-cap becomes more electron-withdrawing, there is a decrease of up to ca. 0.3 e with a concurrent increase in the fractional charge on the end-cap. The majority of the charge on the polyynyl fragment is contained on the alkyne moiety adjacent to the metal center in all cases examined. However, if we consider the most structurally similar set of complexes (i.e., R = C$_6$H$_5$, C$_6$H$_4$NH$_2$-*p*, C$_6$H$_4$NO$_2$-*p*), we notice that as the R group becomes more electron-withdrawing, the percentage of charge located on the C(1)≡C(2) acetylene moiety with respect to the total charge on the carbon fragment increases significantly [R = C$_6$H$_4$NH$_2$-*p* (70.77%) < C$_6$H$_5$ (90.81%) < C$_6$H$_4$-NO$_2$-*p* (94.80%)]. This observation is in agreement with the trends in frontier orbital energies of the [(C≡C)$_n$R]$^-$ fragments, as the greater the electron-accepting ability of the nonmetal end-cap, the more the Ru−C(1) bond is polarized toward the polyynyl ligand, and hence the

(23) Sakurai, A.; Akita, M.; Moro-oka, Y. *Organometallics* **1999**, *18*, 3241.

(24) (a) Dehu, C.; Meyers, F.; Brédas, J. L. *J. Am. Chem. Soc.* **1993**, *115*, 6198. (b) Graham, E. M.; Miskowski, V. M.; Perry, J. W.; Coulter, D. R.; Steigman, A. E.; Schaefer, W. P.; Marsh, R. E. *J. Am. Chem. Soc.* **1989**, *111*, 8771.

Table 4. Distribution of π-Charge throughout the Polyynyl Ligand in the Complexes $[Ru\{(C{\equiv}C)_nC_6H_5\}(PH_3)_2Cp]$

	n					
charge (e^-)	1	2	3	4	5	6
$q\pi_1$	0.09	0.12	0.14	0.15	0.16	0.17
$q\pi_2$	−0.15	−0.18	−0.19	−0.19	−0.19	−0.19
$q\pi_3$		0.00	0.02	0.04	0.05	0.05
$q\pi_4$		−0.04	−0.08	−0.09	−0.09	−0.10
$q\pi_5$			−0.03	0.00	0.01	0.02
$q\pi_6$			0.00	−0.05	−0.06	−0.04
$q\pi_7$				−0.04	−0.01	0.00
$q\pi_8$				0.02	−0.03	−0.04
$q\pi_9$					−0.05	0.00
$q\pi_{10}$					0.04	−0.02
$q\pi_{11}$						−0.05
$q\pi_{12}$						0.05
total	−0.06	−0.10	−0.14	−0.16	−0.17	−0.15

more the charge on the metal-bonded alkyne moiety increases.

While a gross charge distribution model is one way to rationalize the properties of the polyynyl complexes, it is impossible to probe structure and reactivity questions deeply without acknowledging the individual contributions made by σ and π components. As demonstrated by the fragment orbital analysis presented above, and by similar work reported elsewhere,[4,11,16] the dominant σ-type contribution arises from the interaction of the metal d_{z^2} type fragment orbital with the orbital of same symmetry on the polyynyl ligand, and thus the C(1) atom has the greatest net negative charge. However, an examination of the charge residing within the π orbitals (denoted π charge, q_π) on each acetylenic carbon center of the polyynyl ligand reveals a trend toward charge alternation in the π cloud along the polyynyl chain with positive charge residing on the odd-positioned carbon atoms [C(1, 3, 5, ...)] and negative charge on the even atoms [C(2, 4, 6, ...)] (Table 4). Some distortions to this pattern is found for the carbon centers of the alkyne moieties adjacent to the phenyl group presumably arising from the $C{\equiv}C{-}C_6H_5$ interactions (Table 4). The π-charge alternation is most pronounced for the systems with electron-withdrawing groups, and in keeping with the polarization argument given above for the gross charge distribution, there is a slight increase (0.02−0.03 e) in the π charge on C(1) and C(2) as the R group is varied from C_6H_5 to $C_6H_4NO_2$-*p*.

Several reactions of polyynyl species with electrophilic reagents have been reported, with addition of the electrophile to C(2) or C(4) being found.[9e,25] The computational results reported here are entirely consistent with this work and taken together suggest that the addition of electrophiles to polyynyl complexes occurs under charge control. Given the significantly larger charge on C(2), protonation of $[Ru(C{\equiv}CC{\equiv}CH)(PPh_3)_2Cp]$ at C(4) is somewhat surprising.[25] The steric bulk of the metal fragment may therefore also play a role in determining the site of attack, and we do not discount the possibility that this latter reaction occurs via preliminary protonation at C(2), giving the alkynylvinyldene cation $[Ru\{C{=}C(H)C{\equiv}CH\}(PPh_3)_2Cp]^+$ being followed by subsequent rearrangement to the suspected butatrienylidene product $[Ru(C{=}C{=}C{=}CH_2)(PPh_3)_2Cp]^+$.

(25) Bruce, M. I.; Hinterding, P.; Tiekink, E. R. T.; Skelton, B. W.; White, A. H. *J. Organomet. Chem.* **1993**, *450*, 209.

Table 5. Bond Lengths Associated with the Metal−Polyynyl Portion of the Radical Cations $[Ru\{(C{\equiv}C)_nC_6H_5\}(PH_3)_2Cp]^+$

	n					
bond (Å)	1	2	3	4	5	6
Ru−C(1)	1.929	1.909	1.904	1.903	1.904	1.905
C(1)−C(2)	1.249	1.257	1.259	1.258	1.259	1.258
C(2)−C(3)		1.326	1.317	1.314	1.313	1.313
C(3)−C(4)		1.240	1.249	1.254	1.254	1.255
C(4)−C(5)			1.326	1.314	1.311	1.309
C(5)−C(6)			1.238	1.248	1.253	1.255
C(6)−C(7)				1.328	1.316	1.312
C(7)−C(8)				1.236	1.246	1.252
C(8)−C(9)					1.330	1.318
C(9)−C(10)					1.285	1.245
C(10)−C(11)						1.331
C(11)−C(12)						1.233
$C(2n)-C_6H_5$	1.400	1.399	1.399	1.404	1.405	1.406

In addition to the effect of the R group, varying the ligands about the metal center may also modulate the electronic structure, and hence the reactivity and redox properties, of these polyynyl complexes. For example, the diynyl complexes $[Ru(C{\equiv}CC{\equiv}CR)(CO)_2Cp]$, which feature strongly electron-withdrawing carbonyl ligands, exhibit less (0.1 e) excess electron density on the diynyl ligand and the nonmetal end-cap. In essence, the CO ligands withdraw the excess negative charge from the acetylide ligand onto the metal fragment. This leads to a lengthening of the Ru−C(1) bond by about 0.01 Å and a decrease in the C(1)≡C(2) bond length by the same amount relative to the phosphine analogue. It follows that the alternation of the π charge along the carbon backbone is also attenuated with a net decrease of 30%, between the CO and PH_3 species. Thus, replacement of the PH_3-supporting ligands by CO has a similar, but opposite, effect to including an electron-withdrawing R group or increasing the length of the polyynyl ligand.

Effects of Oxidation

The oxidation chemistry of diyndiyl complexes has been investigated thoroughly using a combination of synthetic, electrochemical, structural, and spectroelectrochemical techniques.[3] Similar studies of polyynyl complexes are much less advanced and primarily limited to electrochemical measurements.[5c,26] For a *qualitative* understanding of the changes induced by removal of a single electron from these species it is useful to refer to the MO diagrams in Figure 1. Removal of an electron from the HOMO of these species should lead to a reduction in the net repulsive interaction between the metal d_{xz} and d_{yz} orbitals and the π_x and π_y orbitals of the polyynyl ligand. Since the HOMO is largely centered on the polycarbon chain, oxidation should be expected to give rise to a corresponding change in the C−C bonding interactions. The optimized geometries calculated for each of the complexes $[Ru\{(C{\equiv}C)_nC_6H_5\}(PH_3)_2Cp]^+$ ($n = 1-6$) reveal a significant decrease in the Ru−C(1) bond length from ca. 2.00 Å in the neutral species to ca. 1.900 Å in the oxidized form, an increase of 0.01−0.02 Å in the C≡C bond lengths and a 0.02−0.03 Å decrease in the length of the C−C single bonds (Table 5). These structural differences also correlate well with the HOMO structure depicted in Figure 2, in that bond lengths increase where the orbital interactions are bonding and conversely decrease where they are antibonding.

For complexes with $n < 3$, a comparison of the charge distribution in the oxidized and neutral forms indicates that approximately half of the electron lost originates from the metal fragment, with the remainder originating from the polyynyl ligand and the phenyl group. As the length of the polyynyl ligand increases, the carbon ligand becomes the dominant source of the oxidized electron, which is in complete accord with the nature of the HOMO in the neutral species (Figure 2). Thus, for small n there is a significant effect on the Ru−C bond length upon oxidation, as a large part of the electron removed originates from the metal center, and this effect becomes less as the chain is lengthened. The carbon−carbon bond lengths are much less sensitive to the change since the fraction of electron lost is divided over all the carbon centers of the polyynyl ligand.

As a complementary measure of the origin of the oxidized electron, we have calculated the distribution of unpaired electron spin density in the oxidized species, which corresponds to the probability distribution of the radical electron generated upon oxidation of the neutral species. Graphical displays of the spin density in the cationic species show a significant amount of spin density between the C≡C triple bonded carbon centers (Figure 4). The spin density for all these species is in good qualitative agreement with the shape of the orbital generated by the antibonding combination of d_{xz} and π_x (Figure 1, 2), indicating the that remaining unpaired electron is strongly delocalized. In very recent work, a delocalized diynyl radical has been suggested as a reactive intermediate to rationalize the formation of a binuclear ruthenium species with a C_8H_3 bridge following oxidation of [*trans*-Ru(C≡CC≡CSiMe$_3$)Cl(dppe)$_2$].[27] It is important to note that despite the fact that the molecule is fully able to rearrange its structure and thus localize the unpaired electron, this is in fact not observed and the radical remains delocalized. In all cases the unpaired spin density corresponds to the d_{xz} and π_x antibonding pair despite the fact that it is not the HOMO for species with $n > 2$. This is related to the relaxation of the orbitals upon oxidation and the fact that in the neutral species the two highest occupied orbitals are quasi-degenerate.

To investigate the degree to which oxidation induces structural reorganization within the polyynyl chain, and thereby increases the net amount of cumulenic (═C═C═) character in the molecule, we again consider the net bond order associated with the carbon centers of the carbon-rich ligand. In almost all the species examined, oxidation leads to a decrease in the C≡C bonding density and reduction of the C≡C bond order. Only for the $n = 4$ species is any appreciable cumulenic character observed, and even then the effect is localized along the first four carbons, where the net bond order of C(2)−C(3) and C(4)−C(5) bonds increases only slightly (ca. 0.3), indicating at best a minor contribution from the cumulenic form. These small changes are easily rationalized in terms of the fact that the oxidation removes an essentially delocalized electron which only has a minor effect upon any particular C−C bond within the acetylenic backbone. This property is extremely beneficial for the ultimate realization of the goal to employing these types of compounds as molecular scale wires.[12] If a resonant conductance mechanism, which will generate a transient ionic species, acts across a polyynyl wire, the associated conversion of electrical energy to vibrational energy will ultimately cause the wire to fragment. This effect has been found to lead to the molecular desorbtion from Si substrates in STM experiments with organic adsorbates on silicon surfaces.[28] This restriction

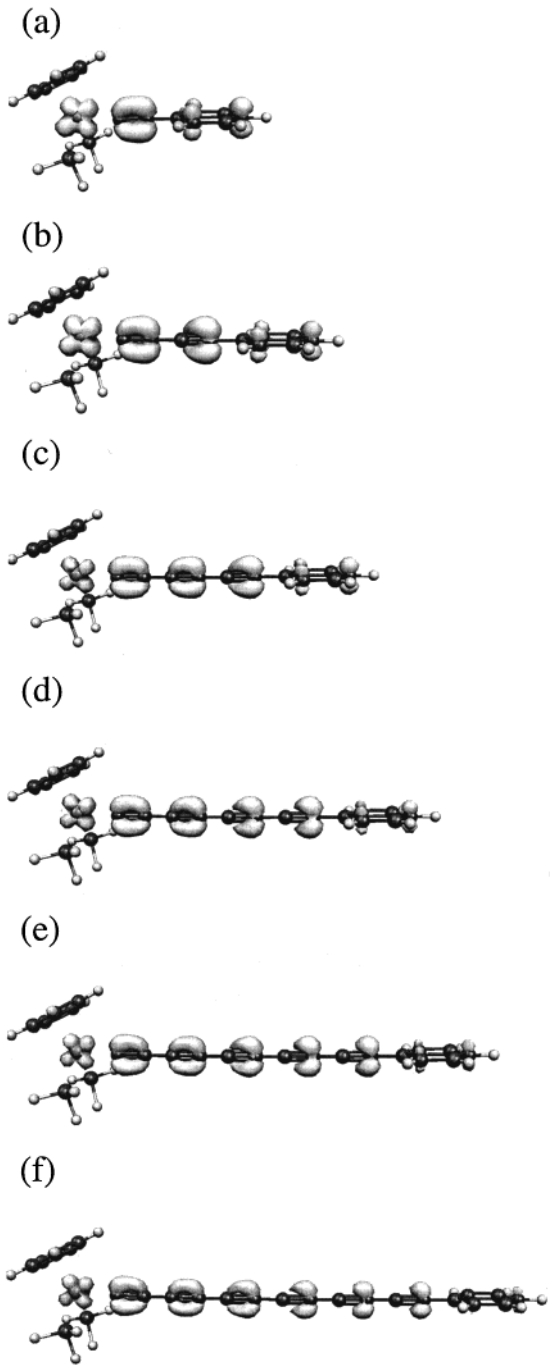

Figure 4. Iso-surface (0.005 au) plot of the computed spin density distribution in the radical cations [Ru{(C≡C)$_n$-C$_6$H$_5$}(PH$_3$)$_2$Cp]$^+$ (n = 1−6).

(26) (a) Wang, W.; Bartik, T.; Brady, M.; Bartik, B.; Ramsden, J. A.; Arif, A. M.; Gladysz, J. A. *J. Am. Chem. Soc.* **1995**, *117*, 11922. (b) Lebreton, C.; Touchard, D.; LePichon, L.; Daridor, A.; Toupet, L.; Dixneuf, P. H. *Inorg. Chim. Acta* **1998**, *272*, 188.

(27) Rigaut, S.; Le Pichon, L.; Daran, J.-C.; Touchard, D.; Dixneuf, P. H. *Chem. Commun.* **2000**, 1206.

(28) Alavi, S.; Rousseau, R.; Lopinski, G. P.; Wolkow R. A.; Seideman, T. *Faraday Discuss.* **2000**, ***117***, 213.

may be surmounted by employing species that show little geometric rearrangement upon change in oxidation state, such as the polyynyl species described in this work.

Conclusion

Our study indicates that the electronic structure of polyynyl complexes is best described in terms of a strong metal−carbon σ bond complimented by a series of filled orbital−filled orbital antibonding π interactions regardless of polyynyl chain length. This supports and extends the conclusions reached about the electronic structure of acetylide complexes and the diynyl complex Fe(C≡CC≡CH)$(CO)_2$Cp described previously.[4f,11] Since the energy of the frontier orbitals of these complexes is related to the degree of σ-donating properties and hence the length of the polyynyl ligand in addition to the nature of the supporting ligands (phosphine vs carbonyl) and the nonmetal end-cap, it should prove possible to tune the redox potentials of these species in a rational manner. This ability to chose oxidation potential has further implications toward energy matching of these wire-like materials to the Fermi level of metallic conductors. The charge distribution along the carbon chain is also susceptible to the nature of the supporting ligands and the electronic properties of the nonmetal end-cap. Since the charge distribution along the carbon ligand suggests a measure of charge control in the reactions of these species and as the range of polyynyl complexes available for reactivity studies increases, subtle differences in reactivity patterns correlated to these factors may become evident. The odd electron in the oxidized species is fully delocalized over the metal and polyynyl ligand, becoming more carbon centered as the length of the polyynyl ligand increases, although the ligand itself retains considerable polyynyl character. Future work from this laboratory will involve ESR and IR spectroelectrochemical investigations of oxidized diynyl and triynyl species such as $[Ru\{(C{\equiv}C)_nC_6H_5\}(PPh_3)_2Cp]^+$ (n = 2, 3) to establish experimental evidence for this claim.

Acknowledgment. This work was carried out with financial assistance from EPSRC and the University of Durham. An NRC summer studentship, University of Durham Postgraduate Scholarship, and Overseas Research Scholarship (O.F.K.) are gratefully acknowledged.

Supporting Information Available: Tables listing computed bond lengths associated with the polyynes $[H(C{\equiv}C)_nH]$ (S1), HOMO−LUMO energies of $[Ru\{(C{\equiv}C)_nR\}(PH_3)_2Cp]$ (R = $C_6H_4NH_2$-*p*, CH_3, H, C_6H_5, $C_6H_4NO_2$-*p*, CN) (S2), fragment charges and total charge distribution for the substituted diynyl complexes $[Ru\{(C{\equiv}C)_2R\}(PH_3)_2Cp]$ (S3), distribution of π-charge throughout the hexynyl ligand in the complexes $[Ru\{(C{\equiv}C)_6R\}(PH_3)_2Cp]$ (R = $C_6H_4NH_2$-*p*, CH_3, H, C_6H_5, $C_6H_4NO_2$-*p*, CN) (S4), computed bond order associated with the hexynyl ligand C−C and C≡C bonds in the substituted complexes $[Ru\{(C{\equiv}C)_6R\}(PH_3)_2Cp]$ (R = $C_6H_4NH_2$-*p*, CH_3, H, C_6H_5, $C_6H_4NO_2$-*p*, CN) and $[H(C{\equiv}C)_6H]$ (S5), total charge distribution in the diynyl carbonyl complexes $[Ru\{(C{\equiv}C)_2R\}(CO)_2Cp]$ (R = $C_6H_4NH_2$-*p*, CH_3, H, C_6H_5, $C_6H_4NO_2$-*p*, CN) (S6), distribution of π-charge throughout the diynyl ligand in the complexes $[Ru\{(C{\equiv}C)_6R\}(L)_2Cp]$ (L = CO, PH_3; R = $C_6H_4NH_2$-*p*, CH_3, H, C_6H_5, $C_6H_4NO_2$-*p*, CN) (S7), fragment charges for $[Ru\{(C{\equiv}C)_nC_6H_5\}(PH_3)_2Cp]^+$ (S8), and net bond order along the carbon chain in the radical cations $[Ru\{(C{\equiv}C)_nC_6H_5\}(PH_3)_2Cp]^+$ (S9).

OM010304+